Evidence for a Catalytic Dyad in the Active Site of Homocitrate Synthase from *Saccharomyces cerevisiae*[†]

Jinghua Qian, Jana Khandogin, Ann H. West, and Paul F. Cook*

Department of Chemistry and Biochemistry, University of Oklahoma, 620 Parrington Oval, Norman, Oklahoma 73019

Received January 16, 2008; Revised Manuscript Received April 3, 2008

ABSTRACT: Homocitrate synthase (acetyl-coenzyme A: 2-ketoglutarate C-transferase; E.C. 2.3.3.14) (HCS) catalyzes the condensation of acetyl-CoA (AcCoA) and α-ketoglutarate (α-KG) to give homocitrate and CoA. Although the structure of an HCS has not been solved, the structure of isopropylmalate synthase (IPMS), a homologue, has been solved (Koon, N., Squire, C. J., and Baker, E. N. (2004) *Proc. Natl. Acad. Sci. U.S.A. 101*, 8295−8300). Three active site residues in IPMS, Glu-218, His-379, and Tyr-410, were proposed as candidates for catalytic residues involved in deprotonation of the methyl group of AcCoA prior to the Claisen condensation to give homocitrylCoA. All three of the active site residues in IPMS are conserved in the HCS from *Saccharomyces cerevisiae*. Site-directed mutagenesis has been carried out to probe the role of the homologous residues, Glu-155, His-309, and Tyr-320, in the *S. cerevisiae* HCS. No detectable activity was observed for the H309A and H309N mutant enzyme, but a slight increase in activity was observed for H309A in the presence of 300 mM imidazole, which is still 1000-fold lower than that of wild type (wt). The E155Q and E155A mutant enzymes exhibited 1000-fold lower activity than wt. The activity of E155A, but not of E155Q, could be partially rescued by formate; a K_{act} of 60 mM with a modest 4-fold maximum activation was observed. In the presence of formate, E155A gives k_{cat}, K_{AcCoA}, and $K_{\alpha\text{-KG}}$ values of 0.0031 s^{-1}, 13 μM, and 39 μM, respectively, while a primary kinetic deuterium isotope effect of about 1.4 was obtained on V, with deuterium in the methyl of AcCoA. The pH dependence of k_{cat} for E155A in the presence of formate gave a pK_a of 7.9 for a group that must be protonated for optimum activity, similar to that observed for the wt enzyme. However, a partial change was observed on the acid side of the profile, compared to the all or none change observed for wt giving a pK_a of about 6.7. The k_{cat} for E155Q decreased at high pH, similar to the wt enzyme, but was pH independent at low pH. The Y320F mutant enzyme only lost 25-fold activity compared to that of the wt, giving k_{cat}, K_{AcCoA}, and $K_{\alpha\text{-KG}}$ values of 0.039 s^{-1}, 33 μM, and 140 μM, respectively, and a primary kinetic deuterium isotope effect of 1.3 and 1.8 on V/K_{AcCoA} and V, respectively; the pH dependence of k_{cat} was similar to that of the wt. These data, combined with a constant pH molecular dynamics simulation study, suggest that a catalytic dyad comprising Glu-155 and His-309 acts to deprotonate the methyl group of AcCoA, while Tyr320 is likely not directly involved in catalysis, but may aid in orienting the reactant and/or the catalytic dyad.

Homocitrate synthase (HCS[1]) (acetylcoenzyme A: 2-ketoglutarate C-transferase; E.C. 2.3.3.14) catalyzes the first and regulated step in the α-aminoadipate pathway for the *de novo* synthesis of L-lysine in fungi (*1, 2*). The α-aminoadipate pathway is unique to euglenoids and higher fungi, which include human pathogens, such as *Candida albicans*, *Cryptococcus neoformis*, and *Aspergillus fumigatus*, and plant pathogens such as *Magnaporthe grisea* (*3, 4*). The uniqueness of the α-aminoadipate pathway makes it a potential target for the design of antifungal drugs.

Homocitrate synthase catalyzes the condensation of AcCoA and α-KG to form homocitrate and CoA. The kinetic mechanism of the enzyme is steady state ordered Bi-Bi with α-KG binding to the enzyme first, followed by acetyl-CoA. After an irreversible hydrolysis of the homocitryl-CoA intermediate, CoA is released prior to homocitrate (*5*).

A chemical mechanism has been proposed for the Zn-containing HCS on the basis of pH-rate profiles, inhibition constants for dead-end analogues, and kinetic isotope effects (Scheme 1) (*6*). α-KG likely binds to enzyme with its α-carboxylate and α-oxo groups coordinated to the active site Zn^{2+}. On the basis of the structure of IPMS, a homologue of HCS, the Zn is also coordinated to two imidazoles, a glutamate, and a water molecule. A general acid and a general base are required for the reaction. The general acid is thought to hydrogen bond to the carbonyl of α-KG and eventually protonate it to form homocitryl CoA. AcCoA then binds with

[†] This work was supported by the Grayce B. Kerr Endowment to the University of Oklahoma (to P.F.C.) and a grant (GM 071417) from the National Institutes of Health (to P.F.C. and A.H.W.).

* Corresponding author: Tel: 405-325-4581. Fax: 405-325-7182. E-mail: pcook@ou.edu.

[1] Abbreviations: HCS, homocitrate synthase; Hc, homocitrate; IPMS, isopropylmalate synthase; wt, wild type; CMS, citramalate synthase; CoA, coenzyme A; AcCoA, acetyl-CoA; α-KG, α-ketoglutarate; α-KIV, α-ketoisovalerate; DCPIP, 2,6-dichlorophenol indolephenol; Mes, 2-morpholinoethanesulfonic acid; Taps, *N*-tris(hydroxymethyl) methyl-3-aminopropanesulfonic acid; Hepes, 4-(2-hydroxyethyl)-1-piperazine-ethanesulfonic acid.

10.1021/bi800087k CCC: $40.75
Published on Web 06/06/2008

Scheme 1: Proposed Chemical Mechanism for Homocitrate Synthase (*6*)

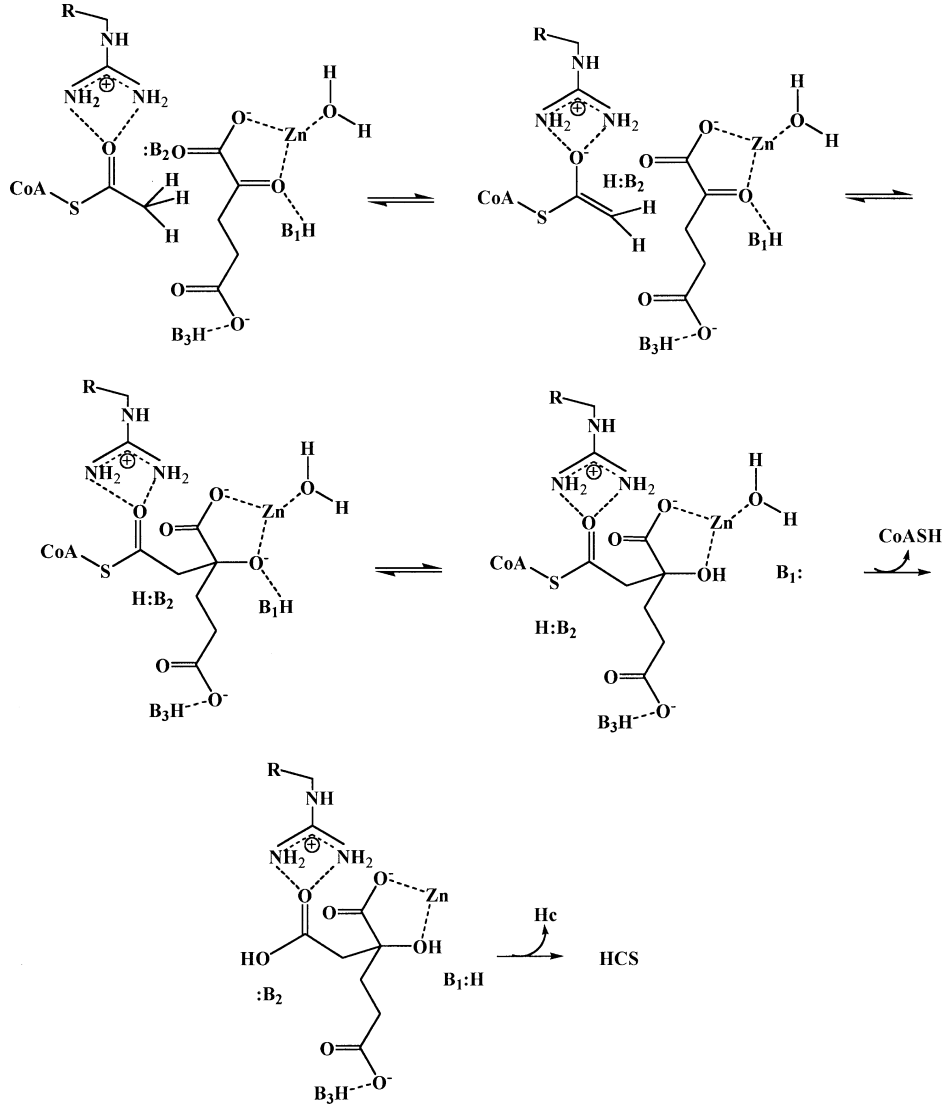

its methyl group positioned near an enzyme residue that will act as a general base. The general base abstracts a proton from the methyl group of AcCoA that will generate the enol (or enolate), which may be stabilized by interacting with a conserved arginine (on the basis of analogy to IPMS). The enolization step, on the basis of primary kinetic deuterium isotope effects, comes to equilibrium prior to the formation of homocitryl-CoA. Nucleophilic attack on the carbonyl of α-KG by the methyl of AcCoA is then carried out, giving the alkoxide of homocitryl-CoA, which then accepts a proton from the general acid. The resulting homocitryl-CoA is hydrolyzed with attack by Zn-OH to give a tetrahedral intermediate, which collapses, likely aided by the general acid acting as a base.

The structure of isopropylmalate synthase (IPMS) from *Mycobacterium tuberculosis*, a homologue of HCS from *S. cerevisiae*, has been solved (*7*), while no structure has yet been solved for an HCS. IPMS and HCS are both Zn-dependent enzymes that catalyze a Claisen condensation between an α-keto acid and AcCoA, and the active site residues in these two enzymes are highly conserved. In the case of IPMS, the substrate is α-ketoisovalerate (α-KIV), while it is α-KG for HCS. The two enzymes share 27% sequence identity and 39% similarity, which suggests the two are related. IPMS has two domains, an N-terminal TIM barrel domain and a C-terminal regulatory domain. The end product leucine binds to the regulatory domain and modulates the activity of the enzyme. The active site is located at the C-terminal end of the TIM barrel domain (Figure 1) and comprises residues from both subunits in the dimer, with H379 and Y410 contributed by one monomer and E218 by the other. The subunit structure of HCS is thought to be similar to that of IPMS, but studies carried out using molecular sieve chromatography were inconclusive and suggested the presence of higher orders species that also had activity (*8*). A cavity adjacent to the binding site for α-KIV was proposed for the AcCoA binding site. Docking AcCoA into the active site placed the methyl thioacetyl of AcCoA between H379, E218, and the C2 atom of α-KIV, with a distance of 3.0−3.5 Å between the methyl of AcCoA and C2 of α-KIV. Y410 is also found in the active site, within hydrogen-bonding distance to E218 (2.4 Å). A possible role as general base was proposed for E218 and/or H379, in deprotonating the methyl of AcCoA to facilitate the condensation reaction. The three active site residues, H379, Y410 and E218, in IPMS are conserved in HCS from *S. cerevisiae* (Figure 2). Site-directed mutagenesis has been carried out to probe the role of these three residues in the *S. cerevisiae* HCS.

To date, the identity of the general acid and general base of HCS is unknown. In this article, site-directed mutagenesis

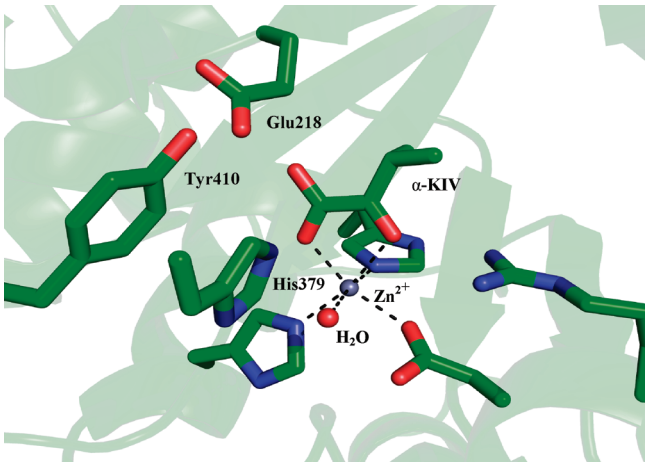

FIGURE 1: Close up view of the active site of isopropylmalate synthase (IPMS) from *Mycobacterium tuberculosis* with α-ketoisovalerate (α-KIV) bound. The figure was prepared using PyMOL version 0.99 (2006) (www.pymol.org). The PDB accession number for the IPMS structure is 1SR9.

was used to change three active site residues, and the resulting mutant enzymes were characterized using initial velocity studies, the pH dependence of the kinetic parameters, and isotope effects. Data combined with a constant pH molecular dynamics simulation study suggest a catalytic dyad, comprising Glu-155 and His-309, functioning as a general base to deprotonate the methyl group of AcCoA.

MATERIALS AND METHODS

Chemicals. α-KG, AcCoA, DCPIP, ammonium formate, and tetramethylammonium hydroxide were obtained from Sigma. Formate, glycerol, KCl, and guanidine hydrochloride were from Fisher Scientific, while $(NH_4)_2SO_4$ was obtained from Fluka. Taps, Hepes, and Mes were from Amresco. Perdeuteroacetic anhydride (98 atom % D) was purchased from Cambridge Isotope Laboratories, Inc. Tetramethylammonium formate was prepared by titrating formic acid with tetramethylammonium hydroxide to neutral pH.

The deuteroacetyl-CoA was prepared as reported previously (*6, 9*). The concentrations of AcCoA and DCPIP stock solutions were adjusted spectrophotometrically, using the following extinction coefficients: AcCoA, $\epsilon_{260} = 16.4$ mM^{-1} cm^{-1} (*10*) and DCPIP, $\epsilon_{600} = 19.1$ mM^{-1} cm^{-1} (*11*).

Cell growth, HCS wt, and mutant enzyme expression, purification and stabilization of the purified enzyme were the same as those reported previously (*8*). Before each assay, 10% glycerol was added to completely dissolve the stabilizing agents in the stock enzyme solution.

Generation of Mutant Enzymes. The H309A, H309N, Y320A, E155A, and E155Q mutant enzymes were prepared using the QuickChange site-directed mutagenesis kit (Stratagene), in accordance with the recommendations of the manufacturer.

Histidine 309 was mutated to alanine utilizing the following forward and reverse primers: $H309A_f$ (5′AAA GCA GGT ATC GCT GCC AAG GCC3′) and $H309A_r$ (5′GGC CTT GGC AGC GAT ACC TGC3′). Mutation to asparagine utilized the following primers: $H309N_f$ (5′ AAA GCA GGT ATC AAT GCC AAG GCC 3′) and $H309N_r$ (5′ GGC CTT GGC ATT GAT ACC TGC 3′). Glutamate 155 was mutated to alanine utilizing the following primers: $E155A_f$ (5′TTT TCC TCT GCA GAT TCC TTC AG3′) and $E155A_r$ (5′CTG AAG GAA TCT GCA GAG GAA AAT C3′), while the E155 to Q mutation utilized the following primers: $E155Q_f$ (5′TTT TCC TCT CAA GAT TCC TTC AG3′) and $E155Q_r$ (5′CTG AAG GAA TCT TGA GAG GAA AAT C3′). The mutation of Y320 to F used the following primers: $Y320F_f$ (5′CCA TCT ACC TTC GAA ATC TTG GAC3′) and $Y320F_r$ (5′GTC CAA GAT TTC GAA GGT AGA TGG3′). Mutated codons are underlined. The nucleotide sequences of the mutant enzymes were confirmed by sequencing the entire mutant gene.

Enzyme Assay. HCS activity was measured using the DCPIP assay developed previously (*8*), monitoring the decrease in absorbance at 600 nm as DCPIP is reduced by CoASH. Reactions were carried out in quartz cuvettes with a path length of 1 cm in a final volume of 0.5 mL containing 50 mM Hepes at pH 7.5, 0.1 mM DCPIP, and variable concentrations of α-KG and AcCoA. Assays were carried out at 25 °C. The activities of all of the mutant and wt enzymes were constant in the absence or presence of 20 μM $ZnCl_2$.[2] For mutant enzyme assays, a control was carried out in the absence of α-KG to correct for nonenzymatic hydrolysis of AcCoA.

pH Studies. The pH dependence of V was obtained by varying AcCoA with the α-KG maintained at a saturating concentration ($10K_m$). The pH was maintained using the following buffers at 100 mM concentration: Mes, 6.0−7.0; Hepes, 7.0−8.0; Taps, 8.0−9.0. The pH was recorded before and after initial velocity data were measured. The enzyme is stable when incubated for 10 min over the pH range 6−9.

Isotope Effects. Primary deuterium isotope effects were measured by direct comparison of initial velocities, where perdeuteroacetyl-CoA was used as the deuterated substrate. Initial rates were measured at different concentrations of AcCoA with α-KG fixed (10 K_m).

Data Analysis. Data were fitted to appropriate equations as discussed below, using the Marquardt−Levenberg algorithm supplied with the EnzFitter program from BIOSOFT, Cambridge, U.K. Kinetic parameters and their corresponding standard errors were estimated using a simple weighting method. Data for formate activation of k_{cat} and initial velocity patterns for HCS wt and mutant enzymes were fitted to eqs 1–2. Data for deuterium isotope effects on V and V/K were fitted using eq 3.

$$\text{app } k_{cat} = \frac{a + \dfrac{\text{formate}}{K_{IN}}}{1 + \dfrac{\text{formate}}{K_{act}}} \quad (1)$$

$$v = \frac{VAB}{K_{ia}K_b + K_a B + K_b A + AB} \quad (2)$$

$$v = \frac{VA}{K_a(1 + F_i E_{V/K}) + A(1 + F_i E_v)} \quad (3)$$

In eq 1, app k_{cat} is the observed k_{cat} at any formate concentration, a is the value of app k_{cat} at zero NH_4^+, K_{act} is

[2] Inhibition was observed at higher concentrations of Zn^{2+}. The activities of all of the mutant and wt enzymes were also unaffected by 1 mM added Mn^{2+}. Mn^{2+} can replace Zn^{2+} in HCS (unpublished results). Zn^{2+} is tightly bound to HCS and does not dissociate upon dialysis.

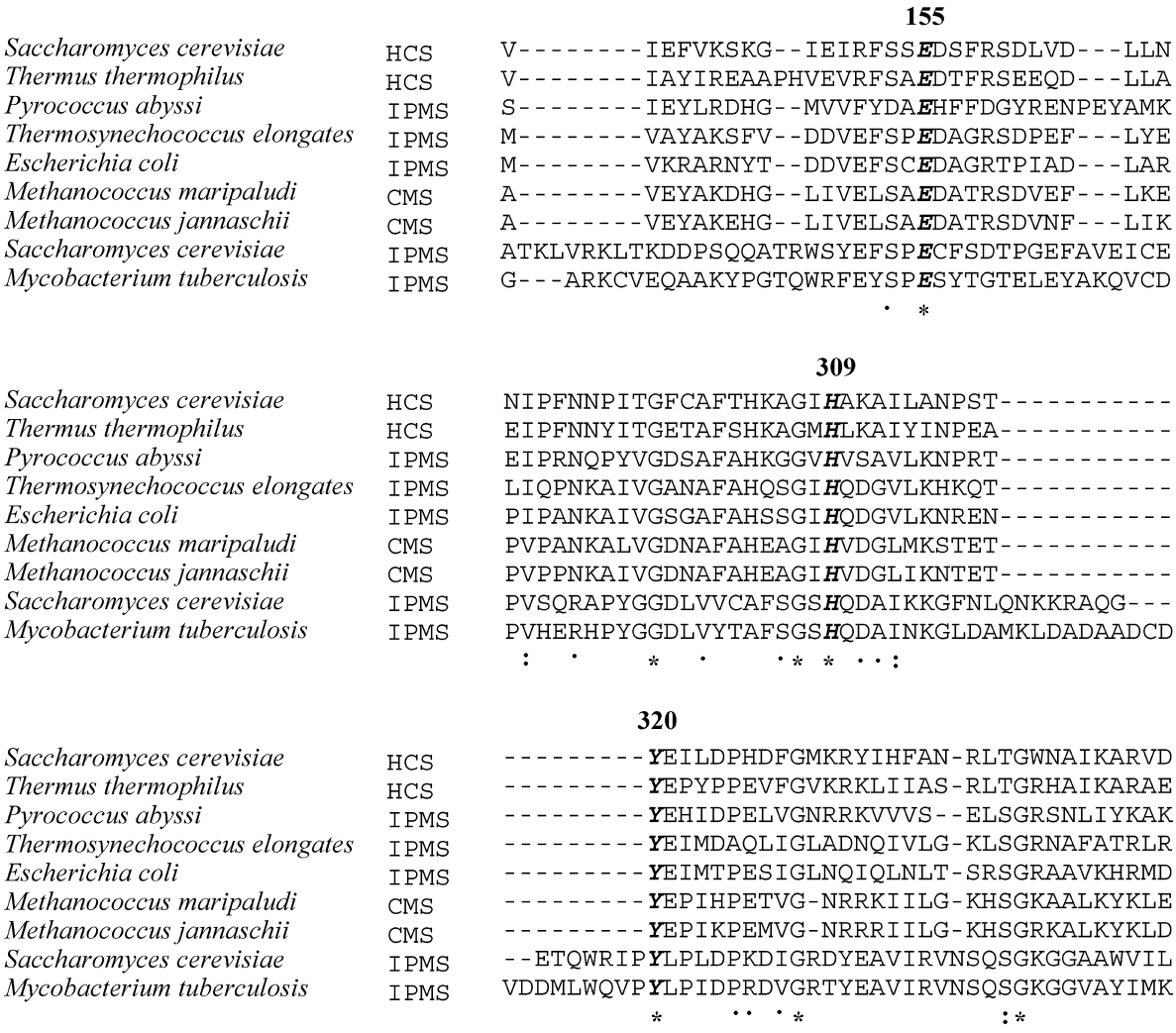

FIGURE 2: Multiple sequence alignment of the residues around E155, H309, and Y320. Homocitrate synthase (HCS), isopropylmalate synthase (IPMS), and citramalate synthase (CMS) all share significant sequence similarity. HCS from *S. cerevisiae* and CMS from *Methanococcus maripaludis* share 30% sequence identity and 53% similarity. The numbering is that of HCS. The alignment was carried out using the program Clustal W. The symbols (*), (:), and (.) indicate the residues in that column that are identical, conserved, and semiconserved, respectively.

the activation constant of formate for the E155A mutant enzyme, and K_{IN} is a ratio of rate constant that causes v to level off at a finite value. In eqs 2 and 3, v is the initial velocity, V is the maximum velocity, $\boldsymbol{A}$ and $\boldsymbol{B}$ are reactant concentrations, K_a and K_b are Michaelis constants for A and B, K_{ia} is the dissociation constants for A, F_i is the fraction of deuterium label in the substrate, and $E_{V/K}$ and E_V are the isotope effects -1 on V/K and V, respectively.

Data for pH-rate profiles that decreased with a slope of 1 at low pH and a slope of -1 at high pH were fitted to eq 4, while data for pH-rate profiles with a partial decrease at low pH and a slope of -1 at high pH were fitted to eq 5.

$$\log y = \log \frac{C}{1 + \frac{\boldsymbol{H}}{K_1} + \frac{K_2}{\boldsymbol{H}}} \tag{4}$$

$$\log y = \log \frac{Y_L\left(1 + \frac{K_2}{\boldsymbol{H}}\right) + Y_H\frac{\boldsymbol{H}}{K_1}}{1 + \frac{\boldsymbol{H}}{K_1}} \tag{5}$$

In eqs 4 and 5, K_1 and K_2 represent acid dissociation constants for enzyme or reactant functional groups, respectively, y is the value of the parameter observed as a function of pH, C is the pH-independent value of y, Y_H and Y_L are the pH-independent values of y at high pH and low pH, respectively, for the E155A mutant enzyme in the presence of formate, and $\boldsymbol{H}$ is the hydrogen ion concentration.

Molecular Dynamics Simulations. Although the overall similarity between HCS and IPMS is only 39%, the active sites are highly conserved. This includes the ligands to the active site Zn^{2+} and all of the proposed catalytic residues. An estimate of the pK_a values was thus sought for IPMS using molecular dynamics simulations to provide some idea of the pK_a values in HCS. The simulations provide information on the pK_a values of the members of the proposed catalytic dyad in a conserved active site. Replica-exchange (REX) continuous constant pH molecular dynamics (CPHMD) simulations were performed with a model of IPMS using the CHARMM program package (version 34) (*12*) and MMTSB tool set (*13*). In constant pH molecular dynamics, protein conformational dynamics is coupled to the protonation equilibria of ionizable groups in a continuum solvent model and a proton bath that represents the external pH condition (*14, 15*). A REX protocol was applied to enhance the sampling of conformational and protonation states (*16*).

The model protein was a truncated version of IPMS (PDB ID: 1SR9), comprising residues 51 to 369 from the N-terminal domain of the first monomer and residues 322 to 429 from the linker domain of the second monomer. The N-terminus was capped with an acetyl group, while the C-terminus was amidated. The truncation allows for a reduction in computational expense and ensures the convergence of conformational and protonation state sampling. It does not affect dynamic and electrostatic properties of the active site residues, Glu218, His379, and Tyr410, and the surrounding region.

Simulations were performed at pH 2, 4, 6, 8, and 10. At each pH, a REX titration simulation was carried out using 32 replicas occupying exponentially spaced temperature windows from 300 to 450 K. Each replica was subjected to constant NVT molecular dynamics using a time step of 2 fs and an identical starting conformation. Replicas adjacent in temperature were allowed to exchange spatial and titration coordinates based on the Monte-Carlo criterion at a 1-ps interval. Titrations included the side chains of Asp, Glu, His, and Tyr residues with model compound pK_a values of 4.0, 4.4, 6.5 (6.6 for N-δ and 7.0 for N-ϵ), and 9.6, respectively. Ionic strength was not included in simulations. Data was collected after 1 ns (per replica) simulation. The relative populations of the unprotonated state of a titrating group were plotted against simulation pH values. The resulting curve was fitted to the generalized Henderson−Hasselbach equation to determine the pK_a value. A correction −0.2 was applied to the computed pK_a value for histidines (*16*).

RESULTS

Initial Velocity Studies. No detectable activity was observed for the H309A and H309N mutant enzymes in the absence or presence of added Zn^{2+} at 0.022 mM mutant enzyme, 50 mM α-KG, and 0.2 mM AcCoA. However, slight activity was observed for H309A in the presence of 300 mM imidazole, giving a lower limit of 0.0011 s^{-1} for the k_{cat} value compared to a value of 1.05 s^{-1} for wt. Activity was too low to characterize the mutant enzyme further. Higher concentrations of imidazole induced hydrolysis of AcCoA and therefore were not tested; 25% of the AcCoA was hydrolyzed in 300 mM imidazole in 1 min.

The E155A and E155Q mutant enzymes exhibited very low activity with k_{cat} values around 0.001 s^{-1}. The activity of E155A, but not E155Q, could be partially rescued by the addition of formate. Formate gave no effect on K_{AcCoA} and $K_{\alpha\text{-KG}}$. A plot of the k_{cat} measured for the E155A mutant enzyme as a function of formate concentration is shown in Figure 3[3]; a K_{act} of 60 mM is estimated for formate. Initial velocity studies of E155A in the presence of 200 mM formate were measured with α-KG varied at different fixed concentrations of AcCoA. Values of k_{cat}, K_{AcCoA}, and $K_{\alpha\text{-KG}}$ were 0.0031 s^{-1}, 13 μM, and 39 μM, respectively (Table 1). (Wild type data are included for comparison.)

Initial velocity studies of the Y320F mutant enzyme give k_{cat}, K_{AcCoA}, and $K_{\alpha\text{-KG}}$ values of 0.039 s^{-1}, 33 μM, and 140 μM, respectively (Table 1).

[3] A value of 0.0019 s^{-1} is shown at 200 mM formate, lower than the value of 0.0031 s^{-1} reported in Table 1. The discrepancy arises from an older enzyme preparation used to collect the data shown in Figure 3. The fold activation was identical for both preparations.

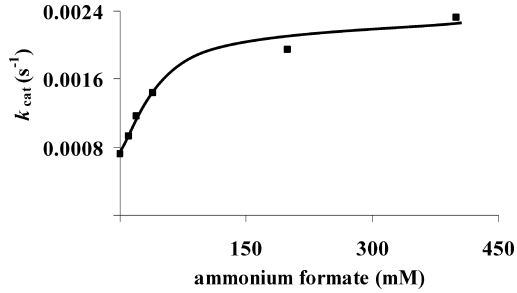

FIGURE 3: Dependence of k_{cat} for E155A on the concentration of ammonium formate. Points are experimental, while the curve is theoretical, on the basis of a fit to eq 1.

Table 1: Summary of the Kinetic Parameters for HCS Wild Type and Mutant Enzymes[a]

	wt	E155A[b]	Y320F
V/E_t (s^{-1})	1.05 ± 0.01	0.0031 ± 0.0003[c]	0.039 ± 0.004
fold decrease		300	25
$K_{\alpha\text{-KG}}$ (mM)	0.14 ± 0.04	0.039 ± 0.016	0.14 ± 0.07
K_{AcCoA} (μM)	42 ± 1	13 ± 4	33 ± 8
$V/K_{\alpha\text{-KG}}E_t$ (M^{-1} s^{-1})	(7.5 ± 2.1) × 10^3	79 ± 33	278 ± 142
$V/K_{AcCoA}E_t$ (M^{-1} s^{-1})	(2.5 ± 0.1) × 10^4	39 ± 12	(1.2 ± 0.3) × 10^3

[a] The K_m values reported previously ($K_{\alpha\text{-KG}}$ = 3.3 ± 0.2 mM, K_{AcCoA} = 2.4 ± 0.2 μM) (*5*) differ significantly from those reported here. Differences are a result of differences in ion concentration in the assay. HCS is activated by monovalent ions such as K^+ and Na^+ (*17, 18*). [b] E155A in the presence of 200 mM formate. These studies were carried out prior to varying formate concentrations. [c] The apparent k_{cat} in the absence of formate was around 0.001 s^{-1}.

pH-Rate Profiles. The pH dependence of k_{cat} for the E155A mutant enzyme in the presence of saturating formate compared to that of the wt enzyme is shown in Figure 4A. The maximum velocity decreases at high pH giving a limiting slope of −1 and a pK_a value of 7.9, but a change of only about 6-fold is observed on the acid side of the profile giving a pK_a of about 7.1. The pH independent value of k_{cat} is 0.0041 ± 0.0009 s^{-1}, while the pH independent value of k_{cat} at low pH is 0.0007 ± 0.0002 s^{-1}, and the ratio of the activities of the partial change at high and low pH is 6 ± 2. pK_a values are summarized in Table 2.

The pH dependence of k_{cat} obtained for E155Q is shown in Figure 4B. Because of the low activity of the enzyme, initial rates are at the limits of detection for the DCPIP assay. As a result, data are qualitative. k_{cat} is pH independent at low pH, but decreases at high pH above pH 8. The estimated pH independent value of k_{cat} is 0.001 s^{-1}.

k_{cat} for Y320F decreases at high and low pH, giving pK values of about 7.1 and 7.9 (Figure 2C and Table 2). The pH independent value of k_{cat} is 0.12 ± 0.02 s^{-1}.

Primary Kinetic Deuterium Isotope Effects. A small primary kinetic deuterium isotope effect was observed for the E155A mutant enzyme with saturating formate (^DV = 1.42 ± 0.15, $^D(V/K)$ = 1.9 ± 0.5) and for the Y320F mutant enzyme (^DV = 1.81 ± 0.16, $^D(V/K)$ = 1.37 ± 0.11). Data are summarized in Table 3.

Molecular Dynamics Simulations and Theoretical pK_a Prediction. To delineate the role of the active site residues, Glu-155, His-309, and Tyr-320, in deprotonation of the methyl group of AcCoA in HCS, titration simulations were carried out with a model IPMS structure (Materials and Methods). The calculated pK_a values of the homologous

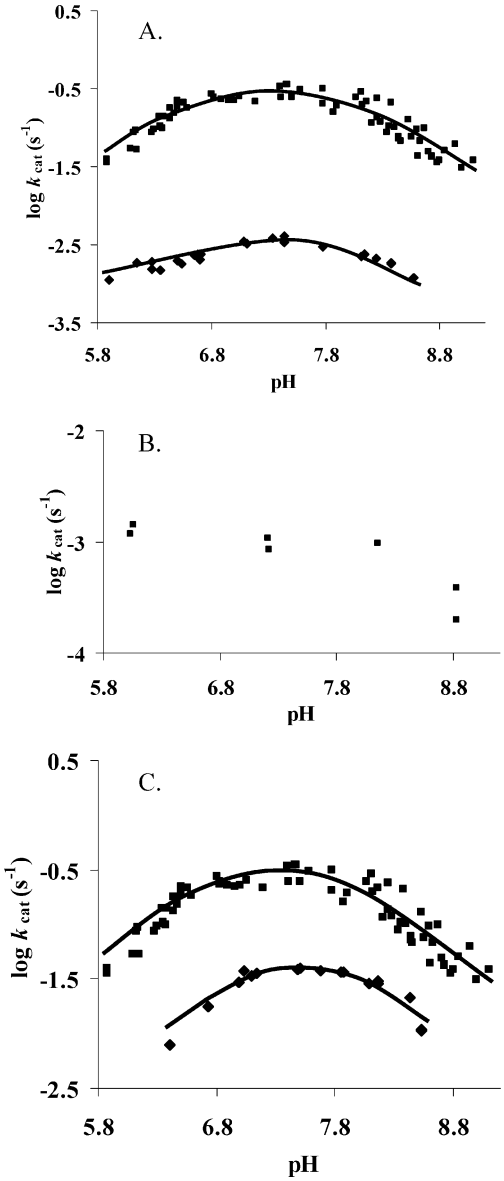

FIGURE 4: pH dependence of k_{cat} for wt and mutant HCS from *S. cerevisiae*. Data were obtained at 25 °C. (A) E155A in the presence of 400 mM of ammonium formate (◆) and wt (■); (B) E155Q; and (C) Y320F (◆) and wt (■). The points shown are the experimentally determined values, while the curves in A and C are theoretical, based on fits of the data using eqs 5 (A(◆)) and 4 (B(■)) and (C(◆ and ■)), respectively.

Table 2: Summary of pK_a Values for wt and Mutant HCS

V_{max}	acidic side pK ± S.E.[c]	basic side pK ± S.E.
wt[a]	6.7 ± 0.2	8.0 ± 0.2
E155A[b]	7.1 ± 0.5	7.9 ± 0.2
Y320F	7.1 ± 0.2	7.9 ± 0.2

[a] Values from ref *6*. [b] E155A plus 400 mM formate. [c] S.E. is standard error.

residues, Glu218, His379, and Tyr410, are reported in Table 4. The pK_a for Glu218 is depressed by 2.8 units, while the pK_a values for His379 and TYR410 are shifted higher by 1.0 and 0.7 units, respectively. The probability distribution for the minimum distance between Glu218 and His379 obtained from molecular dynamics simulations at pH 6 reveals a large conformational cluster around 4 Å (Figure 5). Thus, the charged forms of Glu218 and His379 are

Table 3: Summary of Primary Kinetic Deuterium Isotope Effect Parameters for wt and Mutant HCS at pH 7.2

	^{D}V	$^{D}(V/K)$
wt[a]	1.32 ± 0.11	1.29 ± 0.14
E155A (400 mM formate)	1.42 ± 0.15	1.9 ± 0.5
Y320F	1.81 ± 0.16	1.37 ± 0.11

[a] Values from ref *6*.

Table 4: Summary of Calculated Residue-Based pK_a Values for IPMS

residue	calcd pK_a[a]	standard pK_a
Glu218	1.6	4.4
His379	7.5	6.5[b]
Tyr410	10.3	9.6

[a] Simulations were based on a model IPMS structure, and no ionic strength was included (details see Materials and Methods). [b] Microscopic p$K_a$values of 6.6 for N-δ and 7.0 for N-ϵ were used.

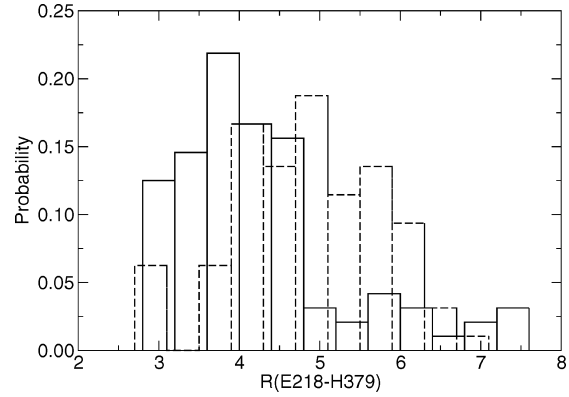

FIGURE 5: Probability distribution for the minimum distance between the carboxylate oxygens of Glu218 and the imidazole nitrogens of His379 observed in molecular dynamics simulations of a model IPMS structure under conditions of pH 6 (—) and pH 8 (---). The histogram width is 0.4 Å.

stabilized by the salt-bridge-like interaction giving rise to significant pK_a shifts, although both residues are completely buried with a solvent accessible surface area of less than 10% (data not shown). The latter desolvation effect contributes to an increase in the pK_a for Glu218 and a decrease in the pK_a for His379 but is apparently weaker than the attractive electrostatic interaction. The simulation at pH 8 shows that, as His379 becomes neutral, the electrostatic interaction with Glu218 weakens (Figure 5). Interestingly, deprotonation mainly occurs at the N-δ atom, while the N-ϵ atom remains protonated and forms a weak hydrogen bond with one of the carboxylate oxygens of Glu218.

Since the residues of interest, Glu218 and His379, are largely buried, we did not employ a Debye−Hückel screening function for effects due to ionic strength, which was estimated to be about 150 mM in the experiment. Also, it should be noted that current simulations employed a Van der Waals surface as the solute−solvent dielectric boundary, which tends to yield a lower desolvation energy (*16*). Taken together, the computed pK_a shifts, especially that for Glu218, may be overestimated, although the direction of the pK_a shifts is reliable as demonstrated by a previous benchmark study (*16*).

DISCUSSION

H309 and E155 Are Important for Catalysis. Changing H309 to A or N gave mutant enzymes with no detectable

Scheme 2: : Proposed Mechanism of AcCoA Enolization via the Catalytic Dyad Comprising His309 and Glu155

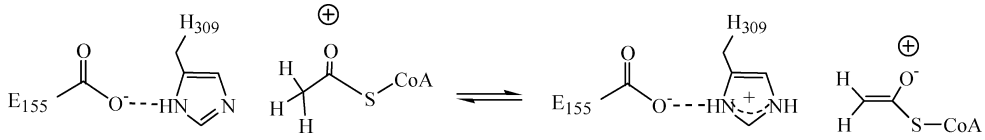

activity. Slight activity was observed for H309A in the presence of 300 mM imidazole.

Replacing E155 with A or Q gave mutant enzymes with 1000-fold lower activity than the wt enzyme. The activity of the E155A, but not the E155Q, mutant enzyme could be partially restored by including formate in the assay solution; no change in the K_m values of α-KG or AcCoA was observed. Measurement of k_{cat} as a function of formate gave a K_{act} for formate of about 60 mM. Activation likely results from formate occupying the vacated E155 carboxylate site, carrying out the role of the carboxylate, albeit with a much reduced efficiency. A maximum activation of about 4-fold was observed at 400 mM ammonium formate. Homocitrate synthase is also activated by monovalent metal ions including Na^+ and K^+, which is similar in size to NH_4^+ (*17, 18*). The activation of E155A by ammonium acetate is only 25% that of ammonium formate, while use of tetramethylammonium formate gave 80% of that with ammonium formate. Data are consistent with the larger acetate being unable to fit into the hole made by eliminating the carboxymethyl group of E155. The remaining 20−25% of the activation observed with ammonium formate and not tetramethylammonium formate is likely due to a slight activation by NH_4^+, which cannot be replaced by the much larger tetramethylammonium ion. Ammonium formate also gave about 25% activation of the wt enzyme, consistent with monovalent cation activation of wt and mutant enzyme by NH_4^+. The concentrations of α-KG and AcCoA used were fixed at 50 mM and 0.2 mM, respectively.

The dramatic loss in activity observed for the H309 and E155 mutant enzymes appears to be due to the removal of the imidazole and carboxlyate side chains and not because of any gross structural changes in the active site. The H309N mutation is expected to be semiconservative since the Asn residue can substitute reasonably well for the His residue in terms of hydrogen-bonding capacity, but the acid−base properties are lost. This is also true of the E155Q mutation.

The E155A mutant enzyme in the presence of saturating α-KG and AcCoA exhibited saturation behavior with respect to formate activation (Figure 1), consistent with the formation of a quaternary E-α-KG-AcCoA-formate complex. Such behavior is not always observed in chemical rescue experiments. In the case of aspartate aminotransferase, the extent of rescue of K258A (K258 is the active site lysine that forms a Schiff base linkage with PLP and acts as a general base once the substrate Schiff base has been formed) by small exogenous amines is directly proportional to the concentration of amine without any hint of rate saturation, suggesting a direct attack by the amine on the solvent exposed face of the external Schiff base (*19, 20*). For HCS, abstraction of a proton from the methyl group of AcCoA by a general base precedes nucleophilic attack by the methyl carbanion on the carbonyl of α-KG. Formate is thus required to bind to the active site, in the cavity created by the mutation prior to the condensation reaction. In order for optimal function of the general base, Glu155 and His309 apparently cooperate, and may function as a catalytic dyad with H309 accepting a proton from the methyl of AcCoA.

pH Dependence of k_{cat}. The pH dependence of k_{cat} is obtained at saturating concentrations of all substrates. The *V* profile will thus reflect ionization of groups within the enzyme−substrate complex required for catalysis (*21*). The *V* pH-rate profile for the wt HCS exhibits slopes of 1 and −1 at low and high pH, respectively, indicating the requirement for one group protonated and another unprotonated for catalysis, likely a general base to catalyze the enolization of AcCoA and a general acid to protonate the α-keto oxygen once the condensation has taken place (Scheme 1) (*6*).

The pH dependence of k_{cat} for E155A in the presence of saturating formate exhibits the requirement for a residue that must be protonated for optimum activity, while a partial change is observed on the acid side of the profile. Thus, the general acid pK_a is unaffected, while the all or none change observed for wt at low pH is replaced by a partial change. The partial change likely reflects titration of the bound formate. Although formate can substitute for the E155 side chain, it is not efficient (the activity of E155A-formate is still only 0.3% that of wt). Protonation of formate gives about a 6-fold decrease in activity, returning enzyme to the unactivated state (1000-fold lower activity than wt). In agreement with this interpretation, the pH-rate profile of k_{cat} for E155Q (which is not activated by formate) shows no pH dependence on the acid side of the profile, but exhibits a decrease in the rate on the basic side.

There are a number of examples of chemical rescue experiments in the recent literature. In (*S*)-mandelate dehydrogenase from *Pseudomonas putida*, it was found that the activity of the H274G mutant enzyme can be rescued by exogenously added imidazoles. The pK_a shifts from a value of 5.1 for H274 in wt to 6.9 for the rescue agent in the pH profiles of the imdazole-rescued H274G mutant enzyme (*22*). In the case of HCS, the pK_a values observed for the wt enzyme and the E155A mutant enzyme bound with formate are very similar. The higher pK_a of formate, compared to its solution pK_a of about 4, likely reflects hydrogen bonding to H309.

Kinetic parameters for the Y320F mutant enzyme (Table 1) show a decrease of about 25-fold in k_{cat}. The pH-rate profile for Y320F is similar to that of wt with the only difference being an increase in the general base pK_a by about 0.4 pH units (7.1 compared to 6.7), but these are equal within error. As a result, Y320 is not essential for catalysis. Given its proximity to the dyad in IPMS, it may aid in orienting the reactant and/or the catalytic dyad.

Primary Kinetic Deuterium Isotope Effects. For the E155A mutant enzyme in the presence of saturating formate, a small primary kinetic deuterium isotope effect was observed using deuteromethyl AcCoA as the labeled substrate; values of 1.42 ± 0.15 and 1.9 ± 0.5 were estimated for ^DV and $^D(V/K)$, respectively. Given the large error on $^D(V/K)$, these values

are likely similar, especially given the large decrease in the value of k_{cat}. The values are similar to those obtained for wt (*6*). Data suggest two possible explanations. Although E155 facilitates the reaction, likely by increasing the basicity of H309, the effect of removing E155 is likely seen as a decrease in the amount of the enolate of the thioester prior to condensation. Alternatively, the effects may reflect the kinetic isotope effect for a late transition state for the enolization step. It is likely that polarization of the thioester carbonyl will be similar for wt and mutant enzymes, which suggests that the first of the two alternative explanations is more likely.

A primary kinetic deuterium isotope effect was also observed for Y320F mutant enzyme with values of 1.81 ± 0.16 and 1.37 ± 0.11 for ^{D}V and $^{D}(V/K)$, respectively. The larger effect on V suggests a contribution to rate-limitation from the enolization step. The smaller isotope effect on V/K_{AcCoA} compared to V suggests some substrate stickiness. The structural differences between the Y320F mutant enzyme and the wt enzyme will have to await the determination of an HCS structure, but must be related to positioning of the thioester of the substrate and H309/E155.

His309 and Glu155 Form a Catalytic Dyad to Act as a General Base. On the basis of the findings discussed above and the crystal structure of the close homologue IPMS, it is suggested that H309 and E155 function as a catalytic dyad to deprotonate the methyl group of AcCoA (Scheme 2). As a result of the hydrogen bond between E155 and H309, the proton affinity of the imidazole should increase, making it a more efficient base, capable of accepting a proton from the methyl of AcCoA. The pK_a of the methyl group of AcCoA is comparable to that of acetone (p$K_a \sim 20$) (*23, 24*). In citrate synthase, the enolization of AcCoA catalyzed by D375 is the rate-limiting step in the reaction, which differs from the mechanism proposed for HCS and IPMS (*6, 25*). The histidine−glutamate dyad acting as the general base in HCS may bring the enolization step to equilibrium prior to condensation. This requires that the pK_a for H309 be increased and that of the methyl of AcCoA be decreased so that they approach one another. The carbonyl of AcCoA is thought to be in hydrogen-bonding distance to a positively charged arginine, which could significantly polarize the ester bond and stabilize the enolate. The result would be a decrease in the pK_a for the methyl protons of AcCoA. The pK_a of about 7 observed for H309/E155 is largely determined by E155. The suggested mechanism is in agreement with constant pH molecular dynamics simulations based on the structure of IPMS, a homologue of HCS with a conserved active site, which suggest a strong electrostatic/hydrogen bond interaction between H309 and E155 and significant up- and downward pK_a shifts for H309 and E155, respectively.

REFERENCES

1. Tucci, A. F., and Ceci, L. N. (1972) Homocitrate synthase from yeast. *Arch. Biochem. Biophys. 153*, 742–750.
2. Gray, G. S., and Bhattacharjee, J. K. (1976) Biosynthesis of lysine in *Saccharomyces cerevisiae*: properties and spectrophotometric determination of homocitrate synthase activity. *Can. J. Microbiol. 22*, 1664–1667.
3. Xu, H., Andi, B., Qian, J., West, A. H., and Cook, P. F. (2006) The α-aminoadipate pathway for lysine biosynthesis in fungi. *Cell Biochem. Biophys. 46*, 43–64.
4. Johansson, E., Steffens, J. J., Lindqvist, Y., and Schneider, G. (2000) Crystal structure of saccharopine reductase from *Magnaporthe grisea*, an enzyme of the α-aminoadipate pathway of lysine biosynthesis. *Structure 8*, 1037–1047.
5. Andi, B., West, A. H., and Cook, P. F. (2004) Kinetic mechanism of histidine-tagged homocitrate synthase from *Saccharomyces cerevisiae*. *Biochemistry 43*, 11790–11795.
6. Qian, J., West, A. H., and Cook, P. F. (2006) Acid-base chemical mechanism of homocitrate synthase from *Saccharomyces cerevisiae*. *Biochemistry 45*, 12136–12143.
7. Koon, N., Squire, C. J., and Baker, E. N. (2004) Crystal structure of LeuA from *Mycobacterium tuberculosis*, a key enzyme in leucine biosynthesis. *Proc. Natl. Acad. Sci. U.S.A. 101*, 8295–8300.
8. Andi, B., West, A. H., and Cook, P. F. (2004) Stabilization and characterization of histidine-tagged homocitrate synthase from *Saccharomyces cerevisiae*. *Arch. Biochem. Biophys. 421*, 243–254.
9. Simon, E. J., and Shemin, D. (1953) The preparation of S-succinyl coenzyme A. *J. Am. Chem. Soc. 75*, 2520.
10. Dawson, R. M. C., Elliott, D. C., Elliott, W. H., and Jones, K. M. (1991) *Data for Biochemical Research)*, 3rd ed., pp 116−117, Oxford University Press, New York.
11. Basford, R. E., and Huennekens, F. M. (1955) Studies on Thiols. I. Oxidation of thiol group by 2,6-dichlorophenol indophenol. *J. Am. Chem. Soc. 77*, 3873–3877.
12. Brooks, B. R., Bruccoleri, R. E., Olafson, B. D., States, D. J., Swaminathan, S., and Karplus, M. (1983) Charmm: A program for macromolecular energy minimization and dynamics calculations. *J. Comput. Chem. 4*, 187–217.
13. Feig, M., Karanicolas, J., and Brooks, C. L., III. (2004) MMTSB tool set: Enhanced sampling and multiscale modeling methods for applications in structure biology. *J. Mol. Graphics Modell. 22*, 377–395.
14. Lee, M. S., Salsbury, F. R., Jr., and Brooks, C. L., III. (2004) Constant-pH molecular dynamics using continuous titration coordinates. *Proteins 56*, 738–752.
15. Khandogin, J., and Brooks, C. L., III. (2005) Constant pH molecular dynamics simulation with proton tautomerism. *Biophys. J. 89*, 141–157.
16. Khandogin, J., and Brooks, C. L., III. (2006) Toward the accurate first-principles prediction of ionization equilibria in proteins. *Biochemistry 45*, 9363–9373.
17. Andi, B., West, A. H., and Cook, P. F. (2005) Regulatory mechanism of histidine-tagged homocitrate synthase from *Saccharomyces cerevisiae*: I. Kinetic studies. *J. Biol. Chem. 280*, 31624–31632.
18. Andi, B., and Cook, P. F. (2005) Regulatory mechanism of histidine-tagged homocitrate synthase from *Saccharomyces cerevisiae*: II. Theory. *J. Biol. Chem. 280*, 31633–31640.
19. Toney, M. D., and Kirsch, J. F. (1992) Brønsted analysis of aspartate aminotransferase via exogenous catalysis of reactions of an inactive mutant. *Protein Sci. 1*, 107–119.
20. Toney, M. D., and Kirsch, J. F. (1989) Direct Bronsted analysis of the restoration of activity to a mutant enzyme by exogenous amines. *Science 243*, 1485–1488.
21. Cleland, W. W. (1977) Determination the chemical mechanisms of enzyme-catalyzed reactions by kinetic studies. *Adv. Enzymol. Relat. Areas Mol. Biol. 45*, 273–387.
22. Lehous, E. I., and Mitra, B. (1999) (S)-Mandelate dehydrogenase from *Pseudomonas putida*: mutations of the catalytic base histidine-274 and chemical rescue of activity. *Biochemistry 38*, 9948–9955.
23. Karpusas, M., Branchaud, B., and Remington, J. (1990) Proposed mechanism for the condensation reaction of citrate synthase: 1.9-Å structure of the ternary complex with oxaloacetate and carboxymethyl coenzyme A. *Biochemistry 29*, 2213–2219.
24. Lau, S.-M., Brantley, R. K., and Thorpe, C. (1988) The reductive half-reaction in acyl-CoA dyhydrogenase from pig kidney: studies with thiaoctanoyl-CoA and oxaoctanoyl-CoA analogues. *Biochemstry 27*, 5089–5095.
25. Carbalho, L. P. S., and Blanchard, J. S. (2006) Kinetic and chemical mechanism of α-isopropylmalate synthase from *Mycobacterium tuberculosis*. *Biochemistry 45*, 8988–8999.

BI800087K